

## Total Synthesis of Hamigerans and Analogues Thereof. Photochemical Generation and Diels–Alder Trapping of Hydroxy-*o*-quinodimethanes

K. C. Nicolaou,\* David L. F. Gray, and Jinsung Tae

Contribution from the Department of Chemistry and The Skaggs Institute for Chemical Biology, The Scripps Research Institute, 10550 North Torrey Pines Road, La Jolla, California 92037, and Department of Chemistry and Biochemistry, University of California, San Diego, 9500 Gilman Drive, La Jolla, California 92093

Received August 18, 2003; E-mail: kcn@scripps.edu

**Abstract:** A number of naturally occurring substances, including hamigerans, contain ring systems which are fused to an aromatic nucleus. A general and streamlined method for the construction of such benzannulated bi- and polycyclic carbon frameworks has been developed, and its scope and limitations were explored. On the basis of the photoenolization of substituted benzaldehydes and subsequent Diels–Alder (PEDA) trapping of the generated hydroxy-*o*-quinodimethanes, this method was optimized to set the stage for the total synthesis of several naturally occurring members of the hamigeran class. Specifically, the developed synthetic technology served as the centerpiece process for the successful asymmetric synthesis of hamigerans A (2), B (3), and E (7). In addition to the PEDA reactions, several other novel reaction processes are described, including a high-yielding decarbonylative ring contraction and an oxidative decarboxylation of a hydroxyl  $\beta$ -keto ester to afford an  $\alpha$ -diketone. A number of analogues of these biologically active natural products were also prepared by application of the developed technology.

### Introduction

In the preceding paper in this issue,<sup>1</sup> we described a total synthesis of hybocarpone in which a photoenolization/Diels–Alder (PEDA) cascade sequence played a pivotal role. Specifically, this efficient process provided access to a benzocyclohexane derivative which served as a precursor to hybocarpone's monomeric unit. The abundance of such structural motifs in naturally occurring substances<sup>2</sup> and the need to synthesize them in the laboratory gifted us with an opportunity to explore this reaction in detail and to apply it, in its intramolecular version, to the total synthesis of hamigerans A, B, and E (1–4 and 7; Figure 1). Isolated from the poecilosclerid sponge *Hamigera tarangaensis* Bergquist and Fromont (family Achinoidae, syn. Phorbasidae) collected at a depth of 30 m near the Hen and Chicken Islands off the coast of New Zealand, the hamigerans contain within their molecular architectures a substituted benzenoid nucleus which is either fused onto a [4.3.0] or a [5.3.0] bicyclic system featuring a *cis* junction, three or four contiguous stereogenic centers, and an isopropyl group (1–5, hamigerans A, B, and C; Figure 1) or appended to a cyclopentane moiety carrying three stereogenic centers, a carboxylic acid group, and

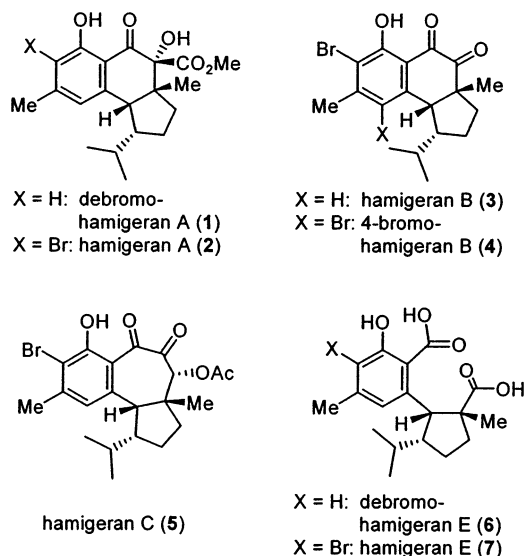
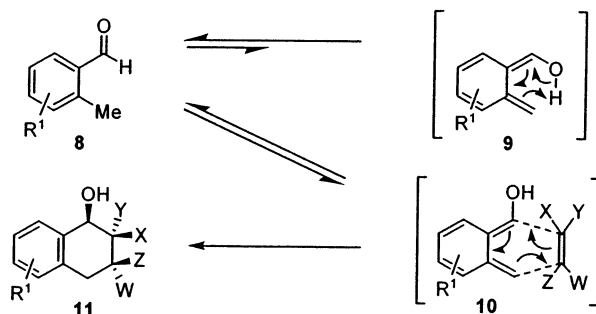


Figure 1. Molecular structures of selected hamigerans (1–7).<sup>1,2</sup>

an isopropyl residue (6, 7, hamigerans E; Figure 1).<sup>3,4</sup> It should be noted that the absolute stereochemistry of hamigeran A (and by extension B and C) has been proposed as shown by structure 2 by X-ray crystallographic analysis.<sup>3,4</sup> The biological properties of these compounds range from moderate cytotoxicity against

(1) Nicolaou, K. C.; Gray, D. L. F. *J. Am. Chem. Soc.* **2004**, *126*, 607–612.  
(2) (a) Kupchan, S.; Morris, S.; Karim, A.; Mareks, C. *J. Am. Chem. Soc.* **1968**, *90*, 5923–5924. (b) Moir, L.; Thompson, R. *J. Chem. Soc., Perkin Trans. 1* **1973**, 1556–1559. (c) Pessoa, L.; De Lemos, T.; De Carvalho, M.; Braz-Filho, R. *Phytochemistry* **1995**, *40*, 1777. (d) Takahashi, M.; Sachihiko, I.; Takahashi, Y. *Bull. Chem. Soc. Jpn.* **1987**, *60*, 2435–2443. (e) Nagahama, S.; Iwaoka, T.; Ashitani, T. *Mokuzai Gakkaishi* **2000**, *46*, 225–230. (f) Jianjun, G.; Guiqi, H.; *Phytochemistry* **1997**, *44*, 759–765. (g) Parish, E. J.; Miles, H. D. *J. Pharm. Sci.* **1984**, *73*, 694–700.

(3) Cambie, R.; Lai, A.; Kernan, M. *J. Nat. Prod.* **1993**, *58*, 940–942.  
(4) (a) Wellington, K.; Cambie, R.; Rutledge, P.; Bergquist, P. *J. Nat. Prod.* **2000**, *63*, 79–85. (b) Cambie, R. C.; Richard, C. E. F.; Rutledge, P. S.; Wellington, K. D. *Acta Crystallogr.* **2001**, *C57*, 958–960.



**Figure 2.** General scheme for the synthesis of diverse bicycles **11** from benzaldehydes **8** employed in the PEDA cascade reaction via hydroxy-*o*-quinodimethanes.

the P-388 leukemia cells [e.g., 4-bromohamigeran **B** (**4**),  $IC_{50} = 13.5 \mu M$ ] to strong antiviral activity against herpes and polio viruses [e.g., hamigeran **B** (**3**), 100% inhibition at  $132 \mu g/disk$ ].<sup>4</sup> Given their scarcity<sup>5</sup> and biological actions, the laboratory synthesis of these molecules was deemed important. In this paper we describe the total synthesis of hamigerans **A** (**1** and **2**), **B** (**3** and **4**), and **E** (**7**), and a number of their analogues, as well as an investigation of the generality and scope of the photoenolization/Diels–Alder reaction, which facilitated the construction of the hybocarpone and hamigeran structural motifs.<sup>6</sup>

## Results and Discussion

**Development of the PEDA Process.** Despite the early discovery of the photoenolization and subsequent Diels–Alder trapping of *o*-methylbenzophenone by Yang and Rivas,<sup>7</sup> the potential of this process in total synthesis remained, for the most part, relatively unexplored. The works of Charlton, Kraus, and Quinkert are notable exceptions, but do not represent a systematic study since they pertain to special circumstances.<sup>8–10</sup> In contrast, the majority of the studies around this so-called photoenolization process deal with its mechanism.<sup>11</sup> Studies had shown that dienol **10** (Figure 2) is a short-lived intermediate which can either relax back to its ground state (i.e., **8**) or be trapped in a Diels–Alder fashion with electron-deficient dienophiles, leading to synthetically useful building blocks.<sup>12–15</sup> It was with this background that we initiated this investigation,

which took special meaning in the context of hybocarpone (intermolecular Diels–Alder trapping) and the hamigerans (intramolecular Diels–Alder trapping). Encouraged by the success of the hitherto unknown PEDA reaction with a 1,1-disubstituted olefin (see preceding paper in this issue),<sup>1</sup> we proceeded to explore the reactivity of a series of activated dienophiles toward benzaldehydes under photolytic conditions as shown in Table 1. While the reaction appeared to be quite general with a variety of substituted benzaldehydes, cyclizing with olefins such as vinyl ketones, acrylate esters, acrylonitriles, and acroleins to afford benzannulated systems, it was noticed that certain dienophiles tended to polymerize rapidly under the photolytic conditions employed. A systematic investigation of reaction variables led to the identification of satisfactory conditions for optimum results. As can be gleaned from Table 2, the effect of common reaction variables on reaction efficiency was quite pronounced, and yields were improved substantially from initial attempts (e.g., entries 1 and 2, Table 2). Thus, by employing an excess of the polymerizable dienophiles, performing the reactions in dilute toluene solution, and using ordinary Pyrex vessels (as opposed to quartz glass), these reactions proceed efficiently as shown in Table 1. It was also found that in going from the parent 2-methylbenzaldehyde (**12**; entry 1, Table 1) to more substituted and electron-rich substrates, the efficiency of the reaction improved substantially (entries 2 and 3, Table 1). This trend appears to be general across a range of dienophiles and benzaldehydes as demonstrated by the more electron-rich substrates corresponding to entries 3, 5–9, and 11–15 (Table 1). Aldehyde **16** also carries a methoxy substituent *ortho* to the aldehyde which might stabilize the dienol species (e.g., **10**; Figure 2) and increase the efficiency with which the fleeting hydroxy-*o*-quinodimethane intermediate is captured.<sup>12d</sup> We were pleased to find that commercially available 3-fluoro-2-methylbenzaldehyde (entry 10, Table 1) reacted with methyl vinyl ketone to afford the corresponding bicyclic fluoride in high yield under the developed photolytic conditions. An example of a double PEDA reaction is also included in Table 1 (entry 17) in which a pentacyclic benzenoid system was produced, albeit in low yield. It should also be noted that several of the reported PEDA reactions represent new ground since they involve hitherto unutilized-in-this-process dienophiles such as cyclopentenone, acrylonitriles, and 1,1-disubstituted olefins, leading to polycycles, nitrile products, and quaternary centers, respectively (entries 4 and 17, 7 and 12, and 6, 8, and 14, Table 1).

In further investigations, attempts were made to employ the Narasaka–Mikami catalyst [(*R*)-BINOL]TiCl<sub>2</sub><sup>16</sup> to obtain PEDA products enriched in one enantiomer. This effort proved largely unsuccessful, although at relatively high catalyst loading, measurable *ee*'s could be obtained (e.g., entry 1, Table 3). Given the fleeting nature of the hydroxy-*o*-quinodimethane intermediate, the lack of profound enantioselection in this process is not surprising.<sup>11a</sup> Furthermore, the diastereoselectivity observed in these PEDA reactions is not spectacular either, with the ratio between *endo* and *exo* Diels–Alder products ranging between 1.5:1 and 8:1 (see Table 1).

The PEDA method is not without limitation. Thus, electron-withdrawing groups on the aromatic nucleus block the produc-

- (5) We gratefully acknowledge Professor R. Cambie for communications pertaining to the hamigerans.
- (6) Nicolaou, K. C.; Gray, D.; Tae, J. *Angew. Chem., Int. Ed.* **2001**, *40*, 3675–3678; Nicolaou, K. C.; Gray, D.; Tae, J. *Angew. Chem., Int. Ed.* **2001**, *40*, 3679–3683. For a recent elegant total synthesis of hamigeran **B**, see: Clive, D. L. J.; Wang, J. *Angew. Chem., Int. Ed.* **2003**, *42*, 3406–3409.
- (7) Yang, N.; Rivas, C. J. *Am. Chem. Soc.* **1961**, *83*, 2213.
- (8) Charlton, J.; Koh, K.; Plourde, G. *Tetrahedron Lett.* **1989**, *30*, 3279–3282.
- (9) (a) Kraus, G.; Zhao, G. *J. Org. Chem.* **1996**, *61*, 2770–2773. (b) Kraus, G.; Chen, L.; Jacobson, R. *Synth. Commun.* **1993**, *23*, 2041–2049.
- (10) Quinkert, G.; Stark, H. *Angew. Chem., Int. Ed. Engl.* **1983**, *22*, 647–655.
- (11) For an overview of this photoenolization process, see: (a) Sammes, P. *Tetrahedron* **1976**, *32*, 405 and references therein. (b) Weedon, A. C. In *The Chemistry of Enols*; Rappoport, Z., Ed.; Wiley: Chichester, U.K., 1990; pp 591–638 and references therein. (c) Charlton, J.; Alauddin, M. *Tetrahedron* **1987**, *43*, 2873–2889 and references therein.
- (12) For early examples of the photoenolization/Diels–Alder reactions with benzylic ketones, see: (a) Haag, R.; Wirz, J.; Wagner, P. *Helv. Chim. Acta* **1977**, *60*, 2595–2607. (b) Pfau, M.; Combrisson, S.; Rowe, J.; Heindel, N. *Tetrahedron* **1978**, *34*, 3459–3468. (c) Nerdel, F.; Brodowski, W. *Chem. Ber.* **1968**, *101*, 1398–1406. (d) Wallace, T. W. Ph.D. Thesis, University of London, 1974.
- (13) For an early example of photoenolization/Diels–Alder reactions with benzaldehydes, see: Arnold, B.; Mellows, S.; Sammes, P.; Wallace, T. J. *Chem. Soc., Perkin Trans. 1* **1974**, *3*, 401–409.
- (14) (a) Charlton, J.; Plourde, G.; Penner, G. *Can. J. Chem.* **1989**, *67*, 1010–1014. (b) Connolly, T.; Durst, T. *Tetrahedron* **1997**, *53*, 15959–15982.
- (15) For a recent review of the Diels–Alder reaction in total synthesis, see: Nicolaou, K. C.; Snyder, S.; Montagnon, T.; Vassilikogiannakis, G. *Angew. Chem., Int. Ed.* **2002**, *41*, 1668–1698.

- (16) Mikami, K.; Motoyama, Y.; Terada, M. *J. Am. Chem. Soc.* **1994**, *116*, 2812–2820.

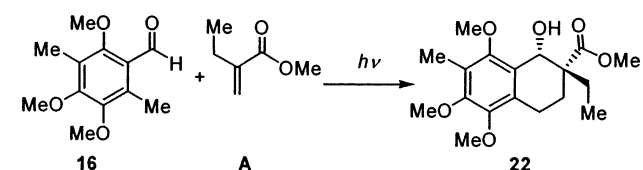
**Table 1.** Benzannulation by Intermolecular Diels–Alder Trapping of Hydroxy-*o*-quinodimethanes Generated via Photoenolization (see Figure 2)<sup>a</sup>

Entry	Aldehyde	Dienophile	Product	t [h]	Yield[%]	Entry	Aldehyde	Dienophile	Product	t [h]	Yield[%]
1				14	53 <sup>b</sup>	10				2	92
2				8	72 <sup>b</sup>	11				2	93
3				4	89	12				6	53 <sup>b</sup>
4				8	71	13				4	84
5				5	82	14				3	82
6				2	89	15				3	8
7				2	75	16				16	53
8				4	83	17				2	16
9				3	84 <sup>b</sup>	[Products were obtained as separable mixtures of diastereoisomers. Major product shown, all products were racemic. See footnotes for product ratios.]					

<sup>a</sup> *o*-Alkylbenzaldehyde (0.5–2 mmol) and olefin (4–20 equiv) were dissolved in deoxygenated toluene (0.03 M) in a Pyrex flask and irradiated at ambient temperature (reactions warmed on irradiation) with a 450 W Hanovia lamp at a distance of 5 cm. Product ratios (*endo:exo*) as follows by entry number: (1) ca. 4:1, (2) ca. 4:1, (3) ca. 3:1, (4) ca. 8:1, (5) ca. 12:4:1, (6) ca. 6:1, (7) ca. 4:1, (8) ca. 2:1, (9) ca. 9:3:1, (10) ca. 8:1, (11) ca. 6:1, (12) ca. 6:3:1, (13) ca. 2:1, (14) ca. 2:1, (15) ca. 2:1, (16) ca. 1.5:1, (17) ca. 2:1. <sup>b</sup> Product ratio determined by NMR spectroscopy.

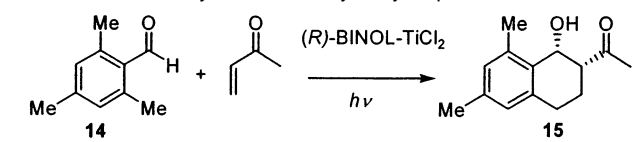
tive pathway to annulated systems (an exception to this general trend is the moderate success of entry 17, Table 1). Halogen and nitro substituents (other than fluorine) were not tolerated

in this reaction. A photocyclization employing a pyridylbenzaldehyde was likewise unsuccessful. While most of the activated olefins tested as competent Diels–Alder partners, vinyl

**Table 2.** Optimization of the Intermolecular Photochemically Induced Diels–Alder Reaction<sup>a</sup>


entry	amt of A (equiv)	concn (M)	$\lambda$ (nm)	temp <sup>b</sup> (°C)	solvent	yield <sup>c</sup> (%)
1	2.0	0.2	260	75	benzene	15
2	2.0	0.2	300	75	benzene	28
3	2.0	0.2	300	75	toluene	38
4	6.0	0.02	300	75	toluene	63
5	6.0	0.02	300	45	toluene	70
6	6.0	0.02	300	45	degassed toluene	83

<sup>a</sup> All reactions were performed by irradiation with a 450 W Hanovia lamp on a 1.0 mmol scale. <sup>b</sup> Internal reaction temperature. The lower temperature was obtained by increasing the distance of the reaction flask from the lamp (3–8 cm). <sup>c</sup> Combined yield of pure compounds. Products were racemic and obtained as a separable mixture (ca. 2:1) of diastereoisomers.

**Table 3.** Effect of (*R*)-BINOL–TiCl<sub>2</sub> on the Diels–Alder Trapping of a Photochemically Generated Hydroxy-*o*-quinodimethane<sup>a</sup>


entry	amt of ( <i>R</i> )-BINOL–TiCl <sub>2</sub> (equiv)	temp (°C)	ee <sup>b</sup> (%)	time (h)	yield (%)
1	0.75	–40	25	12	30 <sup>c</sup>
2	0.05	–40	0	12	20 <sup>d</sup>
3	0.20	25	<5	6	45

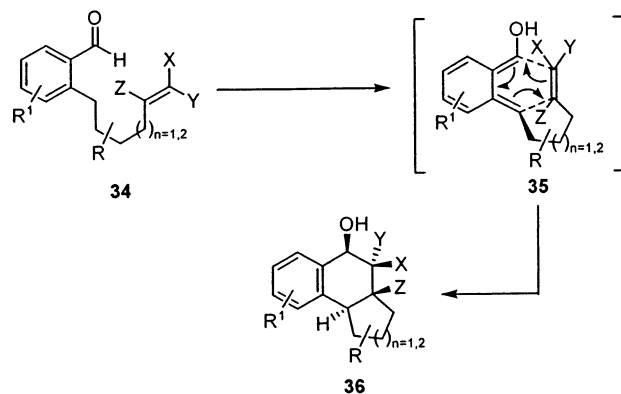
<sup>a</sup> A solution of aldehyde **14** (0.2 mmol), methyl vinyl ketone (4.0 equiv), and (*R*)-BINOL–TiCl<sub>2</sub> were cooled to the indicated temperature and irradiated (450 W Hanovia lamp) in deoxygenated toluene. Workup and chromatography gave pure **15** along with significant amounts of recovered starting material. <sup>b</sup> The enantiomeric excess was measured by chiral HPLC. The absolute configuration was not determined. <sup>c</sup> 30% recovered starting material. <sup>d</sup> 50% recovered starting material.

sulfones and vinyl phosphates failed to give more than trace amounts of PEDAs. Interestingly, while methyl acrylate (entry 13, Table 1), methyl methacrylate (entry 14, Table 1), and 3-penten-2-one (entry 5, Table 1) all reacted with substituted benzaldehyde **16** in high yield to give the expected products, the reaction proved very poor with methyl crotonate (entry 15, Table 1).<sup>17</sup>

It has been determined that the (*Z*)-dienol **9** (Figure 2) is not important in the Diels–Alder chemistry because it can rearrange directly back to the starting material **8** by a 1,5-H shift (the (*E*)-dienol has some small barrier to this rearrangement).<sup>11a</sup> Given that the dienols which are trapped in the PEDAs are exclusively of the (*E*)-dienol type and that the reaction proceeds in a concerted fashion, the stereochemistry-determining facet of this process is the *endo* or *exo* approach of the dienophile to the dienol in the transition state (i.e., **10**, Figure 2).<sup>18</sup> While one might assume *endo* selectivity, a simple

(17) We suspect that a trace contaminant in the commercial formulation of methyl crotonate might be catalyzing rapid decomposition of the dienophile upon photochemical irradiation in this reaction.

(18) Charlton, J.; Plourde, G.; Koh, K. *Can. J. Chem.* **1989**, *67*, 574–579.

**Figure 3.** General scheme for the synthesis of tricycles **36** from substrates **34** via the IMPEDA cascade via hydroxy-*o*-quinodimethanes **35**.

chemical correlation was carried out to confirm this assumption, particularly because NMR (coupling constant analysis and NOE data) was inconclusive for several pairs of isomeric products. The  $\beta$ -hydroxy ester **31** (entry 16, Table 1) was prepared by microbial reduction of the corresponding  $\beta$ -keto ester using the fungus *Mucor racemosus*, which was reported to be *syn*-selective at a level of >99:1.<sup>19–21</sup> From this whole-cell reduction, a single product (**31**) was isolated whose optical rotation matched with the literature value.<sup>20</sup> This compound was, therefore, taken to be the *syn* isomer. The product **31** obtained by the PEDAs reaction (entry 16, Table 1) proved identical to the microbial reduction product by <sup>1</sup>H NMR and <sup>13</sup>C NMR spectroscopy (OH and electron-withdrawing group *syn* to each other). As can be seen from Figure 2, the *syn* isomer is the one which arises from *endo* approach of the dienophile onto the hydroxy-*o*-quinodimethane. On the basis of this result and literature reports,<sup>11</sup> the major reaction products were assigned as the *syn* diastereoisomers.

**Intramolecular Trapping of Photochemically Generated Hydroxy-*o*-quinodimethanes.** As seen in Figure 3, a powerful extension of this benzannulation methodology would be its intramolecular variant (IMPEDA). No example of IMPEDA reaction involving an all-carbon tether between the reacting functionalities (e.g., **34**; Figure 3) had been reported at the outset of this work, and it was clear that the successful implementation of such synthetic technology would provide a useful entry into complex polycycles of the general form **36**.<sup>22</sup> To ascertain the viability of this proposal, we proceeded to access the requisite photocyclization precursors **46a–f**, **47a–f**, **48a–f**, and **52–54** via a general and efficient route (Schemes 1 and 2). Thus, the hydroxy aldehydes<sup>23</sup> **37–39** (Scheme 1) were protected as their dithiane derivatives (BF $\cdot$ OEt<sub>2</sub>, 1,3-propanedithiol, 90–95% yield) and subsequently oxidized with IBX to deliver the aldehydes **40–42** in high yields. The aldehydes so obtained (**40–42**) were then reacted with various commercially available phosphonates (**A–D**; Scheme 1), methylenetriphenylphospho-

(19) Buisson, D.; Cecchi, R.; Laffitte, J.-A.; Guzzi, U.; Azerad, R. *Tetrahedron Lett.* **1994**, *35*, 3091–3094.

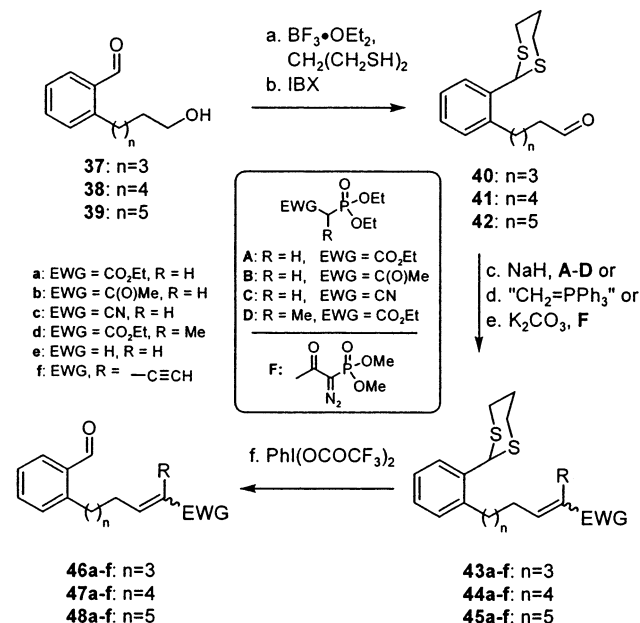
(20) Abalain, C.; Buisson, D.; Azerad, R. *Tetrahedron: Asymmetry* **1996**, *7*, 2983–2996.

(21) We gratefully acknowledge Professor D. Buisson for his generous and timely gift of several fungal and yeast strains used in these experiments.

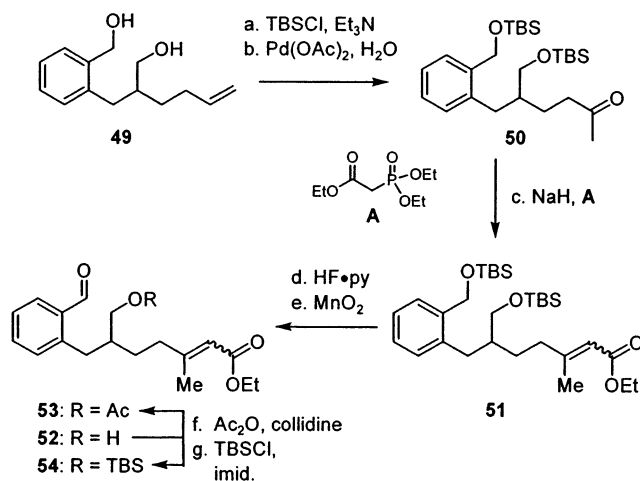
(22) For a report of an intramolecular photocyclization of a benzaldehyde moiety with a heteroatom tether, see: Oppolzer, W.; Keller, K. *Angew. Chem., Int. Ed. Engl.* **1972**, *11*, 728–730.

(23) Huang, Q.; Hunter, J.; Larock, R. J. *Org. Chem.* **2002**, *67*, 3437–3444.



**Scheme 1.** Synthesis of Substituted Benzaldehydes **46a–f**, **47a–f**, and **48a–f** for Intramolecular Photoenolization/Diels–Alder Reactions<sup>a</sup>

<sup>a</sup> Reagents and conditions: (a) BF<sub>3</sub>·OEt<sub>2</sub> (1.0 equiv), CH<sub>2</sub>(CH<sub>2</sub>SH)<sub>2</sub> (1.2 equiv), CH<sub>2</sub>Cl<sub>2</sub>, 0 °C, 1 h, 90–95%; (b) IBX (1.5 equiv), THF–DMSO (1:1), 2 h, 90–95%; (c) NaH (3.0 equiv), phosphonate reagent **A–D** (3.0 equiv), THF, 2 h; then **40**, **41**, or **42** in THF, 25 °C, 2 h, 80–95%; (d) CH<sub>3</sub>PPh<sub>3</sub>Br (3.0 equiv), *n*BuLi (3.0 equiv), THF, –20 °C, 1 h; then **40**, **41**, or **42** in THF, 25 °C, 2 h, 86–93%; (e) K<sub>2</sub>CO<sub>3</sub> (3.0 equiv), phosphonate **F** (1.5 equiv), add **40**, **41**, or **42**, MeOH, –30 to 0 °C, 1 h, 90–93%; (f) PhI(OCOCF<sub>3</sub>)<sub>2</sub> (2.0 equiv) in degassed MeCN–H<sub>2</sub>O (4:1), 0 °C, 0.5 h, 75–90%. IBX = 1-hydroxy-1,2-benziodoxol-3(1*H*)-one 1-oxide.

**Scheme 2.** Synthesis of Functionalized Benzaldehydes **52–54** for Photocyclization<sup>a</sup>

<sup>a</sup> Reagents and conditions: (a) (TBS)Cl (3.0 equiv), Et<sub>3</sub>N (4.5 equiv), CH<sub>2</sub>Cl<sub>2</sub>, 12 h, 94%; (b) Pd(OAc)<sub>2</sub> (0.15 equiv), Cu(OAc)<sub>2</sub> (2.0 equiv), DMA–H<sub>2</sub>O (10:1), O<sub>2</sub> (1 atm), 16 h, 88%; (c) NaH (3.0 equiv), **A** (3.0 equiv), THF, 0–25 °C; then add **50** in THF, 55 °C, 3 h, 89% (3.5:1 *E/Z*); (d) HF·py (6.0 equiv), THF, 25 °C, 40 min, 90%; (e) MnO<sub>2</sub> (20 equiv), CH<sub>2</sub>Cl<sub>2</sub>, 2 h, 87%; (f) Ac<sub>2</sub>O, collidine, 6 h, 74%; (g) (TBS)Cl, imidazole, CH<sub>2</sub>Cl<sub>2</sub>, DMAP(cat.), 12 h, 77%. DMA = *N,N*-dimethylacetamide.

rane, or the Bestmann reagent<sup>24</sup> (**F**; Scheme 1) to furnish the desired olefinic products **43a–f**, **44a–f**, and **45a–f** in good to excellent yields. The dithiane protecting group was then removed [PhI(OCOCF<sub>3</sub>)<sub>2</sub>, 0 °C, 75–90% yield],<sup>25</sup> and the resulting

aldehydes were subjected to fast chromatography, affording substrates **46a–f**, **47a–f**, and **48a–f** (see Scheme 1).

Cyclization substrates **52–54** were prepared according to Scheme 2. Thus, diol **49** was protected as a bis(silyl ether) [(TBS)Cl, Et<sub>3</sub>N, 94%] and then subjected to Wacker oxidation [Pd(OAc)<sub>2</sub>, Cu(OAc)<sub>2</sub>, H<sub>2</sub>O, O<sub>2</sub>] to furnish ketone **50** (88% yield). Horner–Wadsworth–Emmons homologation of this ketone (**50**) with the anion derived from ester phosphonoacetate **A** proceeded smoothly to afford ester **51** as a 3.5:1 mixture of *E/Z* geometrical isomers. The protecting groups were removed from this mixture (**51**) by the action of HF·py in THF to afford a diol which was selectively oxidized at the benzylic position with activated MnO<sub>2</sub> to give the aldehyde cyclization precursor **52**. The remaining free hydroxyl group was protected with acetate (Ac<sub>2</sub>O, collidine) and silyl protecting (TBSCl, imid) groups to deliver substrates **53** and **54**, respectively.

With a collection of suitably substituted benzaldehydes in hand, their photochemical reactions were next investigated. Thus, with the substrates bearing activated olefins connected to the aromatic nucleus with a five- or a six-carbon tether (entries 1–13, Table 4), ultraviolet irradiation (450 W Hanovia lamp, Pyrex filter) at ambient temperature led to a remarkably fast, stereoselective, and efficient ring closure, furnishing the indicated tricycles **56–68** (Table 4) in high yields.

The examples of Table 4 demonstrate the power of this method in constructing both [4.4.0] (entries 1–4) and [4.3.0] (entries 5–13) bicyclic systems which are fused onto aromatic nuclei. Characteristically, the fusion between the two newly formed rings is exclusively *trans*. Furthermore, the substituents on the three contiguous centers C-9, C-10, and C-11 are all *syn* to each other when disubstituted *E* olefins are employed (entries 1–3 and 5–7, Table 4). The results also demonstrate the formation of quaternary centers (entries 4, 8, and 13, Table 4). Limitations of the method include the inability to generate seven-membered rings (e.g., entry 14, Table 4) even after prolonged irradiation, and the failure to accommodate unactivated olefins or alkynes as dienophiles (e.g., entries 15 and 16, Table 4). On the other hand, the reaction performs admirably well with substrate **55** (entry 13, Table 4) carrying a tetrasubstituted activated olefin to afford a product (**68**) with two adjacent quaternary centers, one of which carries a methoxy group. One should also note the tolerance of an acetate or a TBS group within the substrate (entries 10 and 11, Table 4).

Scheme 3 shows a possible transition state for the IMPEDA reaction of **52**. Among the successful IMPEDA examples, entries 9 and 12 (Table 4) shed light on the stereochemical aspects of this process and the possible transition state which leads to the observed outcome. Thus, when (*E*)-**52** (*E* olefin) was irradiated, the *all-syn* product **64** (at C-9, C-10, and C-11; see Scheme 3) was isolated as the major product, with its C-10 epimer [in which the ester group was *anti* to the neighboring two substituents (**67**)] being formed in very small amounts (>25:1 ratio). An *endo* approach of the dienophile onto the reactive diene explains this stereochemical result (transition state, X = CO<sub>2</sub>Et, Y = H; Scheme 3). To our surprise, when pure *Z* olefin (*Z*)-**52** was irradiated under identical conditions, a mixture of the same products (**67**:**64** ratio ca. 3:1) was isolated, with stereoisomer **67** (**64** inverted at C-10) predominating. Assuming a concerted mechanism, this observation requires an *exo*

(24) Mueller, S.; Liepold, B.; Roth, G.; Bestmann, H.-J. *Synlett* **1996**, 6, 521–522.

(25) Stork, G.; Zhao, K. *Tetrahedron Lett.* **1989**, 30, 287–290.

**Table 4.** Synthesis of Tricycles **36** from Substrates **34** through Intramolecular Photoenolization/Diels–Alder Cascade via Hydroxy-*o*-quinodimethanes **35** (See Figure 3)<sup>a</sup>

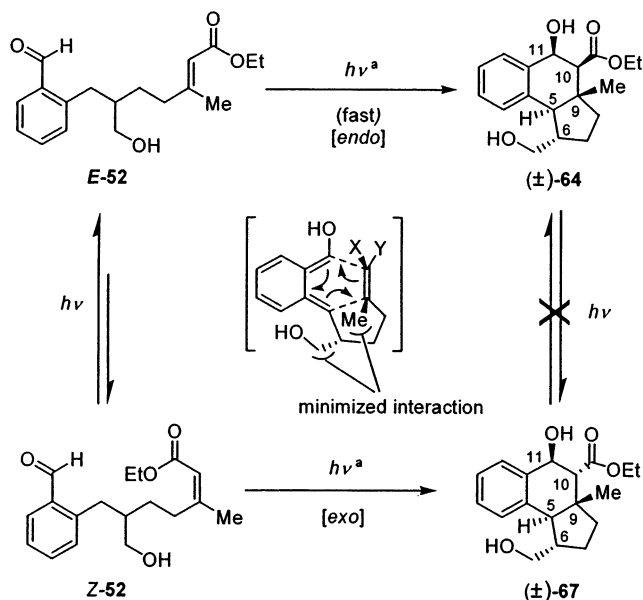
Entry	Aldehyde	Product	t [min]	Yield[%]	Entry	Aldehyde	Product	t [min]	Yield[%]
1			45	94	8			20	92
	<b>47a</b>	<b>56</b>				<b>46d</b>	<b>63</b>		
2			30	92	9			20	94 <sup>(b)</sup>
	<b>47b</b>	<b>57</b>			10	<b>53: R = Ac</b>	<b>65: R = Ac</b>	20	90 <sup>(b)</sup>
					11	<b>54: R = TBS</b>	<b>66: R = TBS</b>	20	93 <sup>(b)</sup>
3			70	81	12			40	89 <sup>(c)</sup>
	<b>47c</b>	<b>58</b>				<b>Z-52</b>	<b>67</b>		
4			45	94	13			60	75 <sup>(d)</sup>
	<b>47d</b>	<b>59</b>				<b>55</b>	<b>68</b>		
5			20	91	14		no cyclization product		
	<b>46a</b>	<b>60</b>				<b>48a</b>			
6			20	90	15		no cyclization product		
	<b>46b</b>	<b>61</b>				<b>47e</b>			
7			45	78	16		no cyclization product		
	<b>46c</b>	<b>62</b>				<b>46f</b>			

<sup>a</sup> *o*-Alkylbenzaldehydes (0.1–0.5 mmol) were dissolved in deoxygenated toluene (0.05 M) in a Pyrex flask and irradiated at ambient temperature (reactions warmed slightly upon irradiation) with a 450 W Hanovia lamp at a distance of 5 cm. Products were obtained as separable mixtures of isomers, the ratio of which was related to be the *E:Z* ratios of the starting olefins. All products were racemic. Starting aldehydes and products shown are the major isomers. <sup>b</sup> Starting olefin, *E:Z* > 25:1; product, C-10 epimers >25:1. <sup>c</sup> Starting olefin, *E:Z* > 20:1; product, C-10 epimers ca. 3:1. <sup>d</sup> Starting olefin, *E:Z* 1.2:1; product, C-10 epimers 2.5:1.

approach (transition state, X = H, Y = CO<sub>2</sub>Et; Scheme 3) of the incoming dienophile onto the hydroxy-*o*-quinodimethane to explain the formation of the major product **67** from (*Z*)-**52**, and an isomerization of olefin geometry under the irradiation conditions to account for the formation of the *all-syn* isomer

**64**. In support of this notion is the fact that the two reaction products **64** and **67** do not interconvert under the reaction conditions. Similarly, irradiation of both (*Z*)-**51** and (*Z*)-**52** in *d*<sub>6</sub>-benzene followed by <sup>1</sup>H NMR spectroscopic analysis demonstrated that olefin isomerization within the starting materials

**Scheme 3.** Stereochemical Course of the Intramolecular Photocyclization with a Substituent at C-6 and the Observed *cis/trans* Isomerization of Reaction Substrate (*Z*)-52



<sup>a</sup> Irradiation of (*E*)-52 Leads Predominantly to 64 in 94% yield (64:67 > 25:1). Irradiation of (*Z*)-52 Leads Predominantly to 67 in 89% yield (67:64 = 3:1).

does occur to a significant extent on the time scale of these processes. Many of the substrates used in these IMPEDA reactions were irradiated as mixtures of *E* and *Z* geometrical isomers, and in most cases the ratios of the two cyclization products (C-10 epimers) were similar to the ratios of isomers in the starting materials. In a few cases [importantly those which took longer to react, including those of entries 12 and 13 (Table 4)], the products (as determined by <sup>1</sup>H NMR spectroscopy) were slightly, but clearly, enriched in the isomer corresponding to the *endo* cyclization of the *E* olefin.

Manual inspection of molecular models confirmed the high strain associated with both the *exo* approach for the *E* isomer [(*E*)-52] and the *endo* arrangement for the *Z* isomer [(*Z*)-52], precluding formation of tricycles with the C<sub>6</sub>-C<sub>10</sub> *syn* junction, which would require such modes of reaction. A final element of stereocontrol is exerted by whatever substituent is placed at the homobenzylic position (C-6) along the tether (transition state, Scheme 3). The products 64 and 67 were obtained as single diastereoisomers with the methyl (C-9) and hydroxymethyl (C-6) groups *anti* to one another. The minimization of steric repulsion between these two groups in the transition state must be responsible for the formation of a single product. This reaction feature raised the possibility of placing a stereocenter at this site (C-6) and using it to template the formation of the remaining four stereocenters in an IMPEDA reaction which would lead to enantiomerically enriched products.

**Initial Forays toward the Total Synthesis of the Hamigerans.** In contemplating potential synthetic routes to the hamigerans, we focused on utilizing the intramolecular trapping of photochemically generated hydroxy-*o*-quinodimethane species as shown retrosynthetically in Figure 4. The methodological developments described above set a strong foundation for this retrosynthetic blueprint. Thus, the hamigeran B series was envisioned to derive from hamigeran A by a decarboxylation/oxidation process (2 → 3, Figure 4). Incidentally, it is interesting

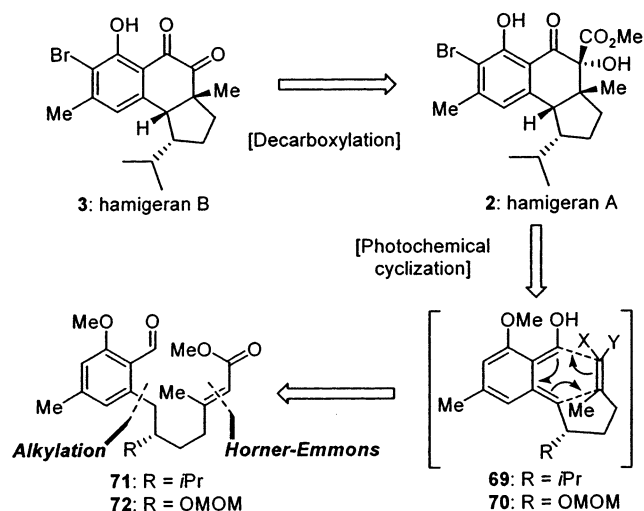


**Figure 4.** Retrosynthetic analysis of the hamigerans 2 and 3 based on the intramolecular trapping of a hydroxy-*o*-quinodimethane (69 or 70).

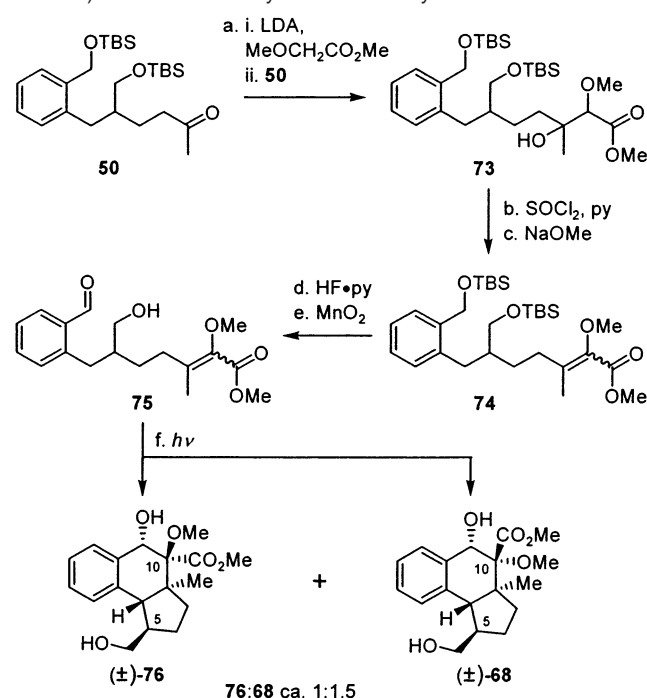
to speculate on the possibility that the entire family of these natural products might arise biosynthetically via interconversion of a few members. The required cyclization precursors 71 and 72 (Figure 4) were to be constructed using standard C–C bond forming reactions. It was anticipated that much of the chemistry employed for the synthesis of the IMPEDA methodology substrates would be directly applicable to the hamigeran synthesis.

An additional cyclization substrate (75; Scheme 4) was prepared as a model system to explore the IMPEDA approach to hamigerans. This was to be a demanding test of the IMPEDA process (vicinal quaternary centers) and an important model study which would shape the hamigeran synthetic route. The requisite substrate 75 was prepared as outlined in Scheme 4. Thus, the previously described ketone 50 (Scheme 2) was added to a solution of the lithium enolate of methyl  $\alpha$ -methoxyacetate at low temperature,<sup>26</sup> leading to the tertiary alcohol 73, obtained as a mixture of diastereoisomers. This crude mixture was treated with SOCl<sub>2</sub> in pyridine followed by exposure to NaOMe (to isomerize nonconjugated elimination products), this sequence affording the tetrasubstituted olefin 74 as an inseparable mixture (ca. 1.5:1) of isomers. Exposure of the latter (74) to HF·py afforded a mixture of diols (not shown, high yield) which was subjected to the action of activated MnO<sub>2</sub> as before to access the targeted intermediate 75 (a ca. 1.5:1 mixture of *E* and *Z* isomers, 79% for two steps, not separated). Irradiation of this mixture provided a ca. 1.5:1 mixture of racemic photocyclization products 76 and 68 (favoring 68) in 76% yield.

At first glance, this was an excellent result, but, upon closer inspection of the reaction products, a problem was uncovered. The surprising outcome of this study was the finding that the major IMPEDA product was 68 with the incorrect stereochemistry at C-10 (and also at C-5 as expected) irrespective of the geometrical ratio of the starting materials (i.e., 75). Despite numerous attempts to separate the *E* and *Z* isomers of the starting aldehydes and irradiate them separately, the 1.5:1 ratio between incorrect and correct C-10 isomers in the product was relatively constant even when the cyclization precursor 75 was enriched

(26) Hiersemann, M.; Lauterbach, C.; Pollex, A. *Eur. J. Org. Chem.* **1999**, *11*, 2713–2724.

**Scheme 4.** Synthesis of Substituted Benzaldehydes **75** (*E* and *Z* Isomers) and Their Photocyclization to Tricycles **68** and **76**<sup>a</sup>



<sup>a</sup> Reagents and conditions: (a) MeOCH<sub>2</sub>CO<sub>2</sub>Me (9.0 equiv), THF, -78 °C; then add LDA (8.0 equiv) over 2 h; then add **50** in THF over 2 h, -78 to 0 °C, 2 h, 90%, mixture of isomers; (b) CH<sub>2</sub>Cl<sub>2</sub>-py (3:1), -50 °C; then add SOCl<sub>2</sub> (10.0 equiv), 15 min, -50 to -20 °C, 2 h, 90%, mixture of isomers; (c) NaOMe (2.0 equiv) in MeOH, 50 °C, 4 h, 85% (1:1.5 *E/Z* mixture, unassigned); (d) HF·py (2.0 equiv), THF, 25 °C, 40 min.; (e) MnO<sub>2</sub> (20 equiv), CH<sub>2</sub>Cl<sub>2</sub>, 25 °C, 2 h, 79% for two steps; (f) *hν*, 450 W Hanovia lamp, Pyrex flask, toluene, ambient temperature, 1 h, 76%. LDA = lithium diisopropylamide.

in one or the other geometrical isomer. The outcome of these experiments might be explained by *E/Z* isomerization of the starting material in a fashion similar to what was observed for (*Z*)-**52** (Scheme 3). This proposal, however, remains unsubstantiated because we were unable to cleanly separate the isomers of **75** (Scheme 4), and because an additional pathway for C-10 epimerization was subsequently discovered (vide infra).

Despite the failure of the first model study to deliver the desired product, the attractiveness of the IMPEDA methodology was too good to abandon, particularly as it appeared ideal for the benzannulated carbocyclic framework found within the hamigeran structures (e.g., **1–4**; Figure 1). The looming obstacle to reaching the hamigerans appeared to be the correct setting of the relative stereochemistry at the contiguous stereocenters situated at C-6, C-5, C-9, and C-10. In a new attempt to solve this problem, two cyclization precursors were designed, one in which the isopropyl group at the C-6 position of the targeted structure **71** (Figure 4) was already installed, and another in which this position was occupied by a protected oxygen functionality (**72**; Figure 4) which could serve as a handle to introduce the obligatory isopropyl group after cyclization, the latter functionality providing the flexibility for epimerization at C-5 at some later stage. Priority was given to the C-5 position in light of the results in Table 2 (all compounds have the undesired *trans* C<sub>5</sub>-C<sub>9</sub> junction). Establishing early on the *trans* relationship between the C-6 isopropyl group and the C-9 methyl substituent was a necessity because these two positions appeared to be inert (toward a possible subsequent correction). In contrast,

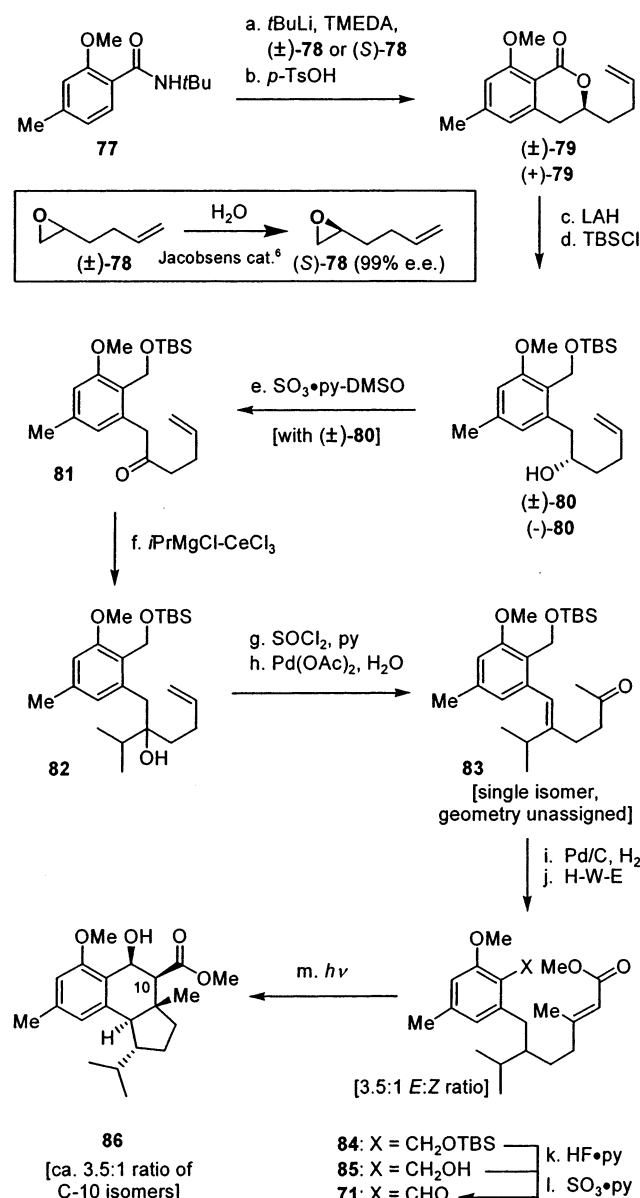
the expected incorrect stereochemistry at the benzylic position (C-5) was considered to be correctable via epimerization due to its potential to be activated under basic, radical, or acidic conditions, coupled with the usual preference for hydrindanes to adopt a *cis* ring junction. The designed substrates **71** and **72** (Figure 4) were destined to be derived from a common intermediate (i.e., **80**) as shown in Scheme 5. For the isopropyl substrate (i.e., **71**), the commercially available racemic epoxide ( $\pm$ )-**78** was utilized as a suitable precursor, whereas, for the protected alcohol substrate (i.e., **72**), enantiomerically enriched (>99% ee) epoxide (*S*)-**78** (obtained via the Jacobsen hydrolytic kinetic resolution method employing the (*S,S*)-cobalt catalyst)<sup>27</sup> was required (vide infra). Thus, to a solution of *tert*-butyl amide **77** (Scheme 5) was added 2 equiv of *t*BuLi (-78  $\rightarrow$  -20 °C) to form the deep-red dianion which opened terminal epoxide ( $\pm$ )-**78** or (*S*)-**78** at -78 °C, leading to a secondary alcohol in 69% yield (Scheme 5).<sup>28</sup> Following crude chromatographic purification, this product was heated in benzene in the presence of *p*-TsOH, causing expulsion of the amide nitrogen moiety by the free secondary hydroxyl group and closure to the  $\delta$ -lactone ( $\pm$ )-**79** or **79** in 91% yield. The latter compound [( $\pm$ )-**79** or **79**] was then reduced with LAH, leading to the corresponding diol, which was selectively monosilylated [(TBS)Cl-Et<sub>3</sub>N, 89% yield] to afford the desired common intermediate ( $\pm$ )-**80** or (-)-**80**. For the series bearing the isopropyl group prior to photocyclization, the more accessible racemic compound was exploited since the integrity of the stereocenter would be lost in the oxidation step. Thus, the free alcohol within ( $\pm$ )-**80** was oxidized (SO<sub>3</sub>·py-DMSO, 94% yield) to afford ketone **81**, which served as a substrate for the installment of the isopropyl group. The addition of *i*PrMgCl to ketone **81** did not occur without prior addition of CeCl<sub>3</sub> to the Grignard reagent to generate the less basic cerium species,<sup>29</sup> which smoothly reacted with the substrate to afford, in 94% yield, tertiary alcohol **82**. Elimination of the tertiary hydroxyl group from the latter compound (**82**) was accomplished in a regioselective fashion by the action of SOCl<sub>2</sub>-py at -50 °C, leading primarily to a single diene (not shown, 80% yield, >10:1 ratio with the alternate geometrical olefin isomer), which was subjected to Wacker oxidation to afford the expected methyl ketone **83** in 81% yield. Hydrogenation (H<sub>2</sub>, 10% Pd/C) of the remaining double bond in the latter compound proceeded smoothly (>95% yield), and the material thus obtained was homologated employing standard conditions [(MeO)<sub>2</sub>P(O)CH<sub>2</sub>CO<sub>2</sub>Me-NaH]. This treatment afforded ester **84** as a ca. 3.5:1 mixture of olefinic isomers (94% combined yield). Desilylation of this substrate (**84**) was accomplished by careful treatment with HF·py in THF (25 °C, 40 min). The final operation in accessing the targeted photocyclization precursor **71** (Scheme 5) was a facile benzylic oxidation initiated by exposure of the latter compound (**85**) to SO<sub>3</sub>·py-DMSO (high yield). Pleasantly, the planned photocyclization occurred as expected, and the tricyclic system **86** was obtained in 91% yield when benzaldehyde **71** (Scheme 5) was irradiated in deoxygenated benzene solution (450 W Hanovia lamp, Pyrex filter). All stereocenters were formed as single

(27) O'Neil, I.; Cleator, E.; Southern, J.; Hone, N.; Tapolczay, D. *Synlett* **2000**, 5, 695–697.

(28) Watanabe, M.; Sahara, M.; Furukawa, S.; Bilodeau, R.; Snieckus, V. *Tetrahedron Lett.* **1982**, 23, 1647–1650.

(29) (a) Imamoto, T.; Takiyama, N.; Nakamura, K.; Hatajima, T.; Kamiya, Y. *J. Am. Chem. Soc.* **1989**, 111, 4392–4398. (b) Takeda, N.; Imamoto, T. *Org. Synth.* **1999**, 76, 228–238.

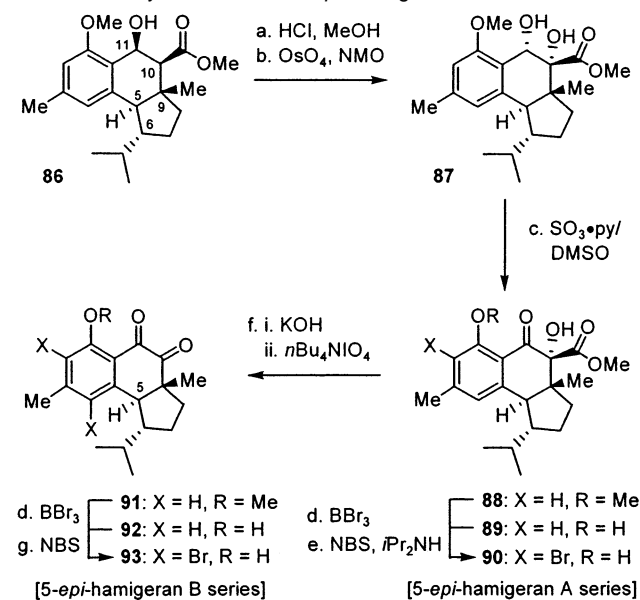


**Scheme 5.** Synthesis of Racemic Aldehyde **71** and Its Photocyclization to **86**<sup>a</sup>

<sup>a</sup> Reagents and conditions: (a) *t*BuLi (2.2 equiv), TMEDA (2.0 equiv), -78 to -20 °C; then ( $\pm$ )-**75** or (*S*)-**75** (1.0 equiv), THF, -78 to 0 °C, 2 h, 69%; (b) *p*-TsOH (2.0 equiv), toluene, reflux, 2 h, 91%; (c) LiAlH<sub>4</sub> (2.0 equiv), THF, 25 °C, 0.5 h, 91%; (d) (TBS)Cl (1.1 equiv), Et<sub>3</sub>N (2.0 equiv), 12 h, 89%; (e) SO<sub>3</sub>•py (3.0 equiv), Et<sub>3</sub>N (6.0 equiv), DMSO-CH<sub>2</sub>Cl<sub>2</sub> (1:1), 0 °C, 2 h, 94%; (f) *i*PrMgCl (2.0 equiv), CeCl<sub>3</sub> (2.0 equiv), -78 to 0 °C, 1 h, 94%; (g) CH<sub>2</sub>Cl<sub>2</sub>-py (3:1), -50 °C; then add SOCl<sub>2</sub> (10.0 equiv), -50 to -20 °C, 0.5 h, 80%; (h) Pd(OAc)<sub>2</sub> (0.1 equiv), Cu(OAc)<sub>2</sub> (2.0 equiv), DMA-H<sub>2</sub>O (10:1), O<sub>2</sub> (1 atm), 16 h, 81%; (i) 10% Pd/C, H<sub>2</sub> (1 atm), NaHCO<sub>3</sub> (solid, 5.0 equiv), EtOAc, 2 h, 95%; (j) (MeO)<sub>2</sub>P(O)CH<sub>2</sub>CO<sub>2</sub>Me (3.0 equiv), NaH (3.0 equiv), THF, 60 °C, 3 h, 94% (mixture of *E/Z* isomers, ca. 3.5:1); (k) HF•py (2.0 equiv), THF, 25 °C, 10 min, 91%; (l) SO<sub>3</sub>•py (3.0 equiv), Et<sub>3</sub>N (6.0 equiv), DMSO-CH<sub>2</sub>Cl<sub>2</sub> (1:1), 0 °C, 2 h, 88%; (m) *h*ν, 450 W Hanovia lamp, Pyrex filter, benzene, 20 min, 91%. MOM = methoxymethyl, and H-W-E = Horner-Wadsworth-Emmons reaction.

isomers except for the expected mixture at C-10 (ca. 3.5:1 ratio), which arises as a consequence of the *E/Z* mixture in the starting material **71**.

With the entire hamigeran ring framework in place in compound **86**, we were now in a position to address the issue of C-5 stereochemistry and the final functional group manipulations required to arrive at the targeted structures. The next

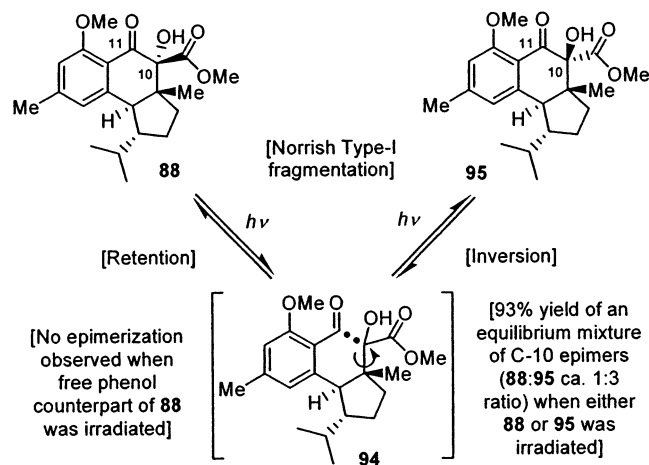
**Scheme 6.** Synthesis of the 5-*epi*-Hamigerans **88–93**<sup>a</sup>

<sup>a</sup> Reagents and conditions: (a) 1% HCl in MeOH, 25 °C, 0.5 h, 90%; (b) OsO<sub>4</sub> (0.1 equiv), NMO (3.0 equiv), THF-*t*BuOH-H<sub>2</sub>O-py (20:20:4:1), 12 h (a ca. 12:1 mixture of isomers), 92%; (c) SO<sub>3</sub>•py (3.0 equiv), Et<sub>3</sub>N (6.0 equiv), DMSO-CH<sub>2</sub>Cl<sub>2</sub> (1:1), 0 °C, 2 h, 88%; (d) BBr<sub>3</sub> (10.0 equiv), CH<sub>2</sub>Cl<sub>2</sub>, -78 °C, 3 h, 96%; (e) NBS (1.05 equiv), *i*Pr<sub>2</sub>NH (0.1 equiv), CH<sub>2</sub>Cl<sub>2</sub>, 0 °C, 3 h, 90%; (f) (i) KOH, MeOH, 70 °C, 2 h; (ii) *n*Bu<sub>4</sub>NIO<sub>4</sub> (2.0 equiv), dioxane, 100 °C, 1 h, 65%; (g) NBS (3.0 equiv), DMF, 25 °C, 3 h, 92%. NMO = 4-methylmorpholine *N*-oxide, and NBS = *N*-bromosuccinimide.

operation was the acid-induced (HCl-MeOH) elimination of water from **86** (Scheme 6), leading to the corresponding conjugated olefin (95% yield), which was then subjected to dihydroxylation with NMO-OsO<sub>4</sub>(cat.) in the presence of pyridine to afford, stereoselectively, diol **87** in 92% yield (ca. 12:1 diastereoselectivity). This sequence makes it obvious that the stereochemistries at C-10 and C-11 in intermediate **86** were inconsequential since both diastereoisomers led smoothly to the same intermediate olefin. At this stage the benzylic position within **87** was oxidized with SO<sub>3</sub>•py-DMSO, leading to the expected hydroxy keto ester **88** (88% yield) whose methoxy group was smoothly cleaved through the action of BBr<sub>3</sub> at -78 °C to afford, in 96% yield, 5-*epi*-debromohamigeran **89**. Attempts to epimerize compound **89** at C-5 as planned under a variety of conditions failed, however, as did experiments intended to bring about the same result with some of its precursors (i.e., the olefinic substrate between **86** and **87** and the keto methoxy derivative **88**). With an efficient route to these compounds, and with an eye for future chemical biology studies, we proceeded to synthesize a number of hamigeran derivatives, albeit epimeric at C-5 (Scheme 6). Thus, selective monobromination *ortho* to the phenolic group in **89** was smoothly effected by following the conditions described by Krohn,<sup>30</sup> which entail the utilization of stoichiometric amounts of NBS and catalytic quantities of *i*Pr<sub>2</sub>NH in CH<sub>2</sub>Cl<sub>2</sub> at 0 °C. This highly regioselective bromination furnished 5-*epi*-hamigeran A (**90**) in 90% yield. Remarkably, omission of the base (*i*Pr<sub>2</sub>NH, 5–10 mol %) in this procedure led to a completely random bromination of the aryl nucleus in **89**. Additional members of the hamigeran family were obtained upon exposure of **88** to base

(30) Krohn, K.; Bernhard, S.; Floerke, U.; Hayat, N. *J. Org. Chem.* **2000**, *65*, 3218–3222.

**Scheme 7.** Postulated Mechanism for the Photochemically Induced Isomerization (Inversion at C-10) of Compounds **88** and **95**



(KOH–MeOH) followed by treatment with  $n\text{Bu}_4\text{NIO}_4$  in dioxane at reflux,<sup>31</sup> a sequence that led to diketone **91** in 65% overall yield from **88**. Cleavage of the methyl ether ( $\text{BBR}_3$ ,  $-78^\circ\text{C}$ ) afforded **92**, which was subjected to aromatic bisbromination by employing an excess of NBS in DMF to provide 5-*epi*-4-bromohamigeran B (**93**) in 94% yield.

Among conditions which were employed in our attempts to invert the C-5 stereochemistry, the irradiation of hydroxy keto ester **88** is of special interest. Thus, upon exposure to light from a UV Hanovia lamp in benzene solution, **88** was converted to an equilibrium mixture of C-10 epimers (**88:95** ratio ca. 1:3; see Scheme 7). A likely reaction course for this equilibration may involve a Norrish type I homolysis<sup>32,33</sup> of the C<sub>10</sub>–C<sub>11</sub> bond to form a fleeting diradical species (**94**) which can either reclose back to **88** or invert its stereochemistry at the radical center prior to recombination, which would lead to the formation of the C-10 epimer **95** (Scheme 7). Notably, no epimerization was observed upon irradiation of compound **89** (Scheme 6), which has a free phenol. If the proposed mechanism is correct, the ketone chromophore plays a central role in this rather unusual but potentially useful transformation.

At this stage, we performed molecular modeling and computational studies which indicated that epimerization of compounds such as **88** (Figure 5) would not be productive.<sup>34</sup> At the same time, these studies suggested that our alternate strategy (delay of isopropyl group installation) could be successful. Thus, it appears that the isopropyl moiety resides in an extremely hindered position. In particular, one of its methyl groups is

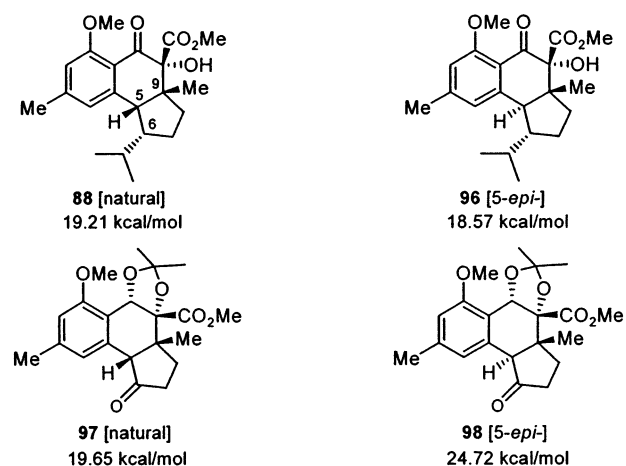


**Figure 5.** Relative strain energies of 6,9-*cis* and 6,9-*trans* hamigeran-type structures **88** and **96**–**98**. See ref 34 for computational parameters.

positioned very near the aromatic ring in computationally minimized structures. This alignment is supported by  $^1\text{H}$  NMR spectroscopic data recorded for **88** in which the two methyl groups are in significantly different chemical environments (chemical shifts at 1.02 and 0.74 ppm). The close interactions of the isopropyl group with the tricyclic portion of the molecule are relieved in the 5-*epi* compounds, which may account for the *trans*-hydrindane being uncharacteristically more stable (by computation) than the natural *cis* isomer (**88** vs **96**; Figure 5). We noted that replacing the isopropyl-group-bearing  $\text{sp}^3$  carbon with an  $\text{sp}^2$  center (such as a carbonyl, **97** and **98**; Figure 5) in the modeling studies had a rather drastic effect on the energy difference between the *cis* and *trans* isomers, with the *cis* isomer now being highly favored (**97** vs **98**; Figure 5). In light of these computational studies and experimental results, we embarked on a second approach to the hamigerans which would proceed through key intermediate **72** (Scheme 8).

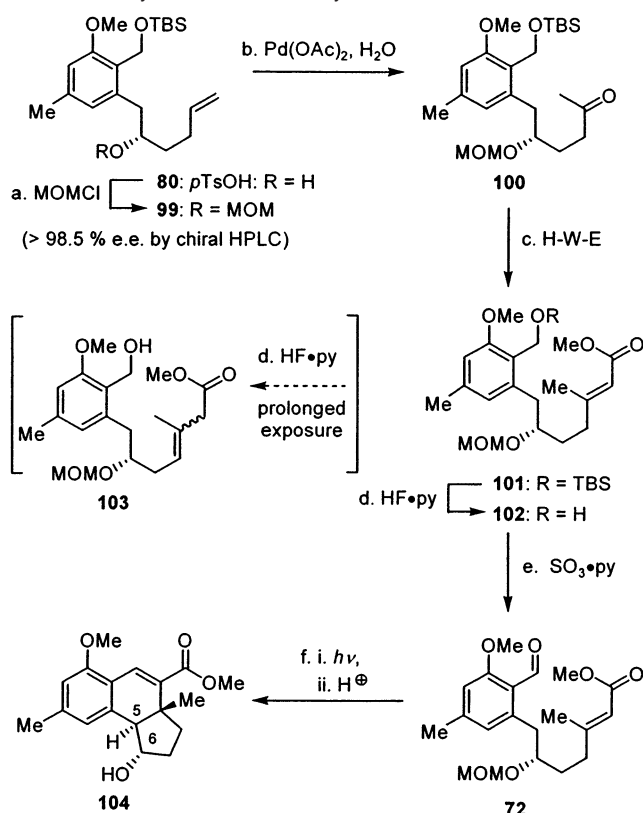
The synthesis of the required compound **72** commenced from the enantiomerically enriched alcohol (–)-**80** (ee > 99%) as shown in Scheme 8. Thus, protection of (–)-**80** as its MOM ether [(MOM)Cl,  $\text{EtNiPr}_2$ , 83% yield] led to derivative **99**, whose Wacker oxidation [ $\text{Pd}(\text{OAc})_2$ ,  $\text{Cu}(\text{OAc})_2$ ,  $\text{H}_2\text{O}$ ,  $\text{O}_2$ ] furnished methyl ketone **100** as the major product (81% yield) together with small amounts of the corresponding aldehyde (9%). Extension of the chain within **100** was carried out as before (see Scheme 5), furnishing the *E*- $\alpha,\beta$ -unsaturated ester **101** as the major product, together with its *Z* geometrical isomer in a ca. 3.5:1 ratio and in 94% combined yield. Desilylation of **101** proved problematic at first, since the olefinic bond was found to rapidly deconjugate to its  $\beta,\gamma$ -unsaturated isomer **103** following removal of the protecting group. The nonconjugated olefin would not return to conjugation under any of the several basic or acidic conditions screened. This side reaction, which was observed to a lesser extent in the isopropyl counterpart of **101**, was finally overcome by employing  $\text{HF}\cdot\text{py}$  in THF at ambient temperature (20 min) for the desilylation step, leading to the desired benzylic alcohol **102** in 91% yield. Oxidation of **102** was cleanly accomplished by exposure to the  $\text{SO}_3\cdot\text{py}$ –DMSO protocol (92% yield), marking our arrival at the second photocyclization precursor **72**. And, gratifyingly, irradiation of this substrate under the developed conditions gave cleanly the expected mixture of C-10 tricyclic epimers in high yield. The crude product so obtained was then treated with 1% methanolic

(31) Santaniello, E.; Ponti, F.; Manzocchi, A. *Tetrahedron Lett.* **1980**, *21*, 2655–2656.

(32) Barltrop, J.; Coyle, J. J. *Chem. Soc. D* **1969**, *19*, 1081–1082.

(33) For recent computational studies on the Norrish type I reaction and further references, see: (a) Diau, E.; Kotting, C.; Zewail, A. *ChemPhysChem* **2001**, *2*, 273–293. (b) Diau, E.; Kotting, C.; Zewail, A. *ChemPhysChem* **2001**, *2*, 294–309.

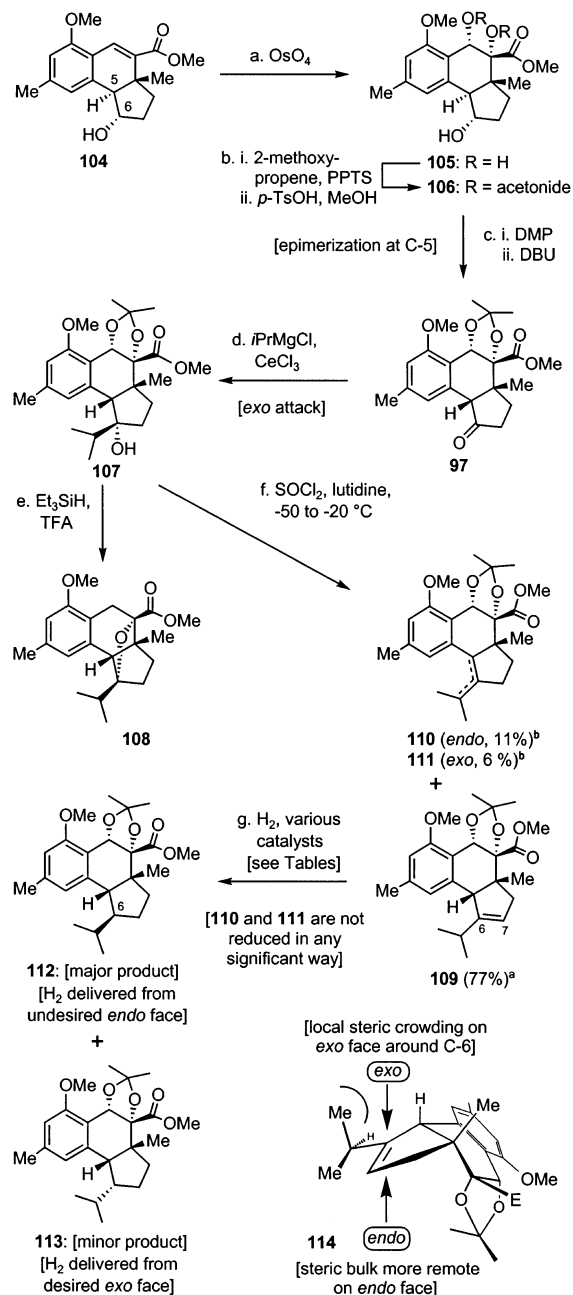
(34) The hamigeran diastereoisomeric pairs were modeled with Accelrys Insight II, 1998. Molecular dynamics calculations were performed with Accelrys Discover v. 2.98 on a cluster of SGI Origin servers running Irix 6.5. The relative energies of the diastereoisomeric were computed with the class II pairwise force field  $\text{cff91 v. 2.0}$  (see: Dinur, U.; Hagler, A. In *Reviews in Computational Chemistry*; Lipkowitz, K., Boyd, D., Eds.; VCH: New York, 1991; Vol. 2, p 527), with library parameters for bond, valence, torsion, and out-of-plane terms. A total of 1000 structures were generated within 300 ps at 800 K. They were annealed to 300 K in 5 ps. The structures were further minimized to convergence using a conjugate gradient algorithm, and the lowest energy structure cluster was selected as the preferred structure. We thank Dr. C. N. C. Boddy for performing these calculations.

**Scheme 8.** Synthesis and Photocyclization of Precursor **72**<sup>a</sup>

<sup>a</sup> Reagents and conditions: (a) (MOM)Cl (2.0 equiv), *i*Pr<sub>2</sub>NEt (6.0 equiv), CH<sub>2</sub>Cl<sub>2</sub>, 25 °C, 12 h, 83%; (b) Pd(OAc)<sub>2</sub> (0.1 equiv), Cu(OAc)<sub>2</sub> (2.0 equiv), DMA–H<sub>2</sub>O (10:1), O<sub>2</sub> (1 atm), 16 h, 81%; (c) (MeO)<sub>2</sub>P(*o*)CH<sub>2</sub>CO<sub>2</sub>Me (3.0 equiv), NaH (3.0 equiv), THF, 60 °C, 3 h, 94% (mixture of *E/Z* isomers, ca. 3.5:1); (d) HF·py (2.0 equiv), THF, 25 °C, 20 min, 91%; (e) SO<sub>3</sub>·py (3.0 equiv), Et<sub>3</sub>N (6.0 equiv), DMSO–CH<sub>2</sub>Cl<sub>2</sub> (1:1), 0 °C, 2 h, 92%; (f) *hν*, 450 W Hanovia lamp, Pyrex filter, benzene, 25 min; then 1% anhydrous HCl in MeOH, 60 °C, 1 h, 85%.

HCl at 60 °C to furnish the desired hydroxyolefin **104** by concomitant elimination of water and cleavage of the MOM group, in 85% overall yield from **72**.

Our next attempt at the total synthesis of the hamigerans utilized the alternate tricycle **104** (Scheme 9), which incorporated an oxygen functionality at C-6, in the hope that this position could be manipulated to give the necessary activation for the required C-5 epimerization. Although less direct, this strategy had the potential to allow for an enantioselective synthesis of the targeted compounds since an enantiopure starting material was employed to synthesize **104**. The efficiency of the synthetic sequence leading to compound **104** facilitated its multigram production with over 99% enantiomeric purity as determined by chiral HPLC. Borrowing from the successful advancement of the isopropyl substrate (see Scheme 6), hydroxyolefin **104** was dihydroxylated with NMO and catalytic OsO<sub>4</sub>, giving triol **105** (94% yield) as shown in Scheme 9. Again, the facial selectivity in this reaction was excellent (ca. 12:1 in favor of **105**), presumably controlled by an approach in which minimum interactions between the reagent and the angular methyl group at the ring junction were encountered. Selective protection of the vicinal hydroxyl groups in **105** was achieved with the combination of 2-methoxypropene and catalytic amounts of PPTS, a reaction that was followed by exposure of the crude product to *p*-TsOH in MeOH (to cleave the somewhat stable hemiketal formed at the C-6 hydroxyl

**Scheme 9.** Correction of the Stereochemistry at C-5 via Base-Induced Epimerization and Elaboration toward the Hamigerans **1–4**<sup>a</sup>

<sup>a</sup> Reagents and conditions: (a) OsO<sub>4</sub> (0.1 equiv), NMO (3.0 equiv), THF–*t*BuOH–H<sub>2</sub>O–py (20:20:4:1), 12 h, 94% (ca. 12:1 diastereoselectivity); (b) (i) 2-methoxypropene (20 equiv), PPTS (0.3 equiv), CH<sub>2</sub>Cl<sub>2</sub>, 0 °C, 0.5 h; (ii) *p*-TsOH (1.0 equiv), MeOH, 0 °C, 0.5 h, 93%; (c) (i) DMP (1.7 equiv), CH<sub>2</sub>Cl<sub>2</sub>, 0 °C, 1 h; (ii) DBU (0.5 equiv), CH<sub>2</sub>Cl<sub>2</sub>, 0 °C, 10 min, 93% for two steps; (d) *i*PrMgCl (2.0 equiv), CeCl<sub>3</sub> (2.0 equiv), –78 to 0 °C, 1 h, 95%; (e) Et<sub>3</sub>SiH (50 equiv), TFA (20 equiv), CH<sub>2</sub>Cl<sub>2</sub>, 25 °C, 1 h, 65%; (f) SOCl<sub>2</sub> (6.0 equiv) py–lutidine–CH<sub>2</sub>Cl<sub>2</sub> (1:5:5), –50 to –20 °C, 2 h, 94%; (g) H<sub>2</sub>, catalyst; see Table 5 for conditions, yields, and product distributions. DMP = Dess–Martin periodinane, PPTS = pyridinium *p*-toluenesulfonic acid, and DBU = 1,8-diazabicyclo[5.4.0]undec-7-ene. <sup>b</sup> Product distributions determined by <sup>1</sup>H NMR spectroscopy.

group), leading to acetonide **106** (93% yield for two steps). Dess–Martin oxidation of the remaining hydroxy group in **106** then gave the corresponding ketone acetonide **98** (see Figure 5) in high yield. With the ketone at the homobenzylic position (C-6), base-induced epimerization at C-5 became facile, requir-

**Table 5.** Attempted *exo* Reduction of Trisubstituted Olefins **109–111**

entry	conditions	product distribution by <sup>1</sup> H NMR spectroscopic analysis (%)			
		110	111	endo-112	exo-113
1	PtO <sub>2</sub> , 3 atm of H <sub>2</sub> , EtOAc, 6 h	6	3	71	20
2	Pd(OH) <sub>2</sub> , 3 atm of H <sub>2</sub> , EtOH, 12 h	24	10	50	15
3	10% Pd/C, 50 atm of H <sub>2</sub> , EtOAc, 6 h	40	7	33	19
4	Rh–Al <sub>2</sub> O <sub>3</sub> , 50 atm of H <sub>2</sub> , EtOH, 48 h	7	3	6	21
5	Rh black, 20 atm of H <sub>2</sub> , EtOH, 48 h	negligible conversion to products			
6	IrP(cyhex) <sub>3</sub> (COD)(py)PF <sub>6</sub> , 10 atm of H <sub>2</sub> , CH <sub>2</sub> Cl <sub>2</sub> , 48 h	negligible conversion to products			

<sup>a</sup> A mixture of olefins (**109–111**, 0.05 mmol) was dissolved in the indicated solvent and stirred under H<sub>2</sub> pressure (Parr bomb) for the indicated times, at which time the catalyst was removed by filtration and product ratios were determined by <sup>1</sup>H NMR spectroscopic analysis.

ing only a brief exposure to DBU at 0° C to afford, in 93% yield for two steps, the desired product **97** with the *cis* [C5–C9] junction. Addition of the reagent formed by mixing *i*PrMgCl and CeCl<sub>3</sub> to ketone **97** proceeded smoothly and stereoselectively to afford tertiary alcohol **107** as a single product (95% yield) through convex (*exo*) face attack.

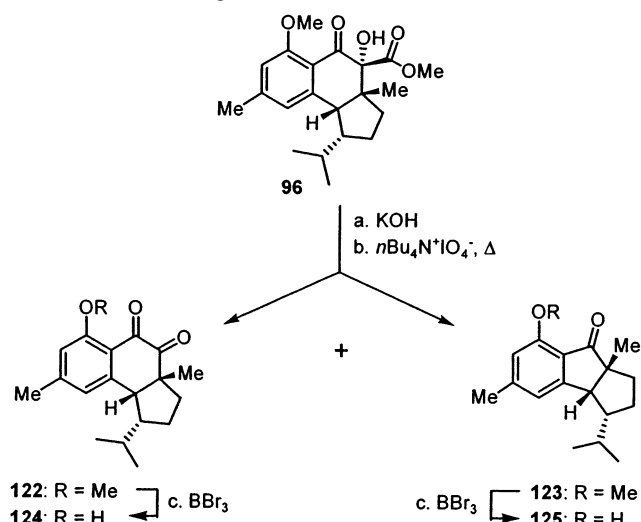
Having installed the entire carbon skeleton of the hamigerans within **107** (see Scheme 9), ways were then sought to excise the extra hydroxyl group at C-6. An attempt to reductively remove the free hydroxyl from **107** by reaction with TFA–Et<sub>3</sub>SiH failed, leading instead to the novel polycyclic ether **108** (65% yield), presumably via acetonide collapse, followed by concomitant trapping of the incipient tertiary carbonium ion by the resulting proximal C-10 hydroxyl group and reductive cleavage of the benzylic C–O bond. The steric hindrance around C-6 is probably responsible for the recalcitrance at this position toward reduction. Nevertheless, conditions were eventually found for the regioselective elimination of this hydroxyl group. Thus, exposure of **107** to SOCl<sub>2</sub>–lutidine–pyridine in CH<sub>2</sub>Cl<sub>2</sub> at –50 to –20 °C resulted in the formation of the trisubstituted olefin **109** as the major product (77% yield) together with small amounts of the tetrasubstituted olefins **110** (11%) and **111** (6%). However, the intended reduction of this olefinic mixture to furnish the desired hamigeran stereochemistry at C-6 as expected from an *exo* face attack [cf. the addition of an isopropyl group to the carbonyl group at C-6 in **97** (**97** → **107**)] proved elusive. Thus, upon hydrogenation, the major product obtained (**112**) exhibited consistently the wrong orientation of the isopropyl moiety, despite the many catalysts and conditions employed (see Table 5). Examination of manual and computational models of **109** raises the possibility that one of the methyl groups from the isopropyl moiety is responsible for this unexpected result as demonstrated by structure **114** (Scheme 9). Nevertheless, the strong preference for hydrogen to be delivered to the *endo* face

of the bicycle is surprising. The entries in Table 5 reveal the unusual reluctance toward hydrogenation that these molecules display, resisting even elevated pressures of hydrogen and highly active catalyst systems. These observations, when taken together with the completely *exo*-selective alkylation of ketone **97** with the bulky isopropyl nucleophile, point to the isopropyl group itself as the dominant stereochemistry-directing force around the C-6 atom, overriding any effects inherent within the fused ring system. The undesired product **112** was isolated together with unreactive (and inseparable) tetrasubstituted olefinic isomers **110** and **111** as well as small amounts of the desired reduction product **113**. The observed distribution of unreacted olefins **110** and **111** was, in some experiments (entries 2 and 3, Table 5), higher than in the starting mixture, suggesting that olefin isomerization was a preferred reaction course under some of the conditions employed. Having reached that far into the sequence, it was decided to complete it with the C-6 epimeric (major isomer) intermediate **112**, with the aim of validating the proposed route to the hamigerans and to obtain analogues of it.

Scheme 10 summarizes these efforts, which culminated in the synthesis of four 6-*epi*-hamigeran analogues, **117–120**. A mixture of **110**, **111**, **112**, and **113** (ca. 6:3:71:20) obtained from reduction of **109–111** according to entry 1 (Table 5; PtO<sub>2</sub>, H<sub>2</sub>) was subjected to the action of 3 M aqueous HCl in THF (1:1) at 80 °C, conditions which not only cleaved the acetonide group but also randomized the benzylic hydroxyl group, complicating the mixture even further. Oxidation of this mixture (SO<sub>3</sub>·py–DMSO), however, resulted in a new mixture from which ketone **116** was chromatographically separated in 45% overall yield from the mixture of **109–111**. Unfortunately, we were unable to isolate any material possessing the correct C-6 stereochemistry at this stage, despite the presence of that isomer (**113**) after the initial hydrogenation step. Demethylation of the phenolic group within **116** with BBr<sub>3</sub> at –78 °C proceeded smoothly, forming



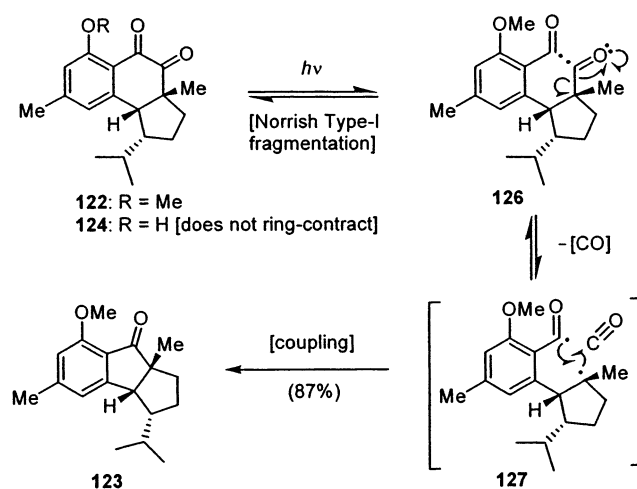
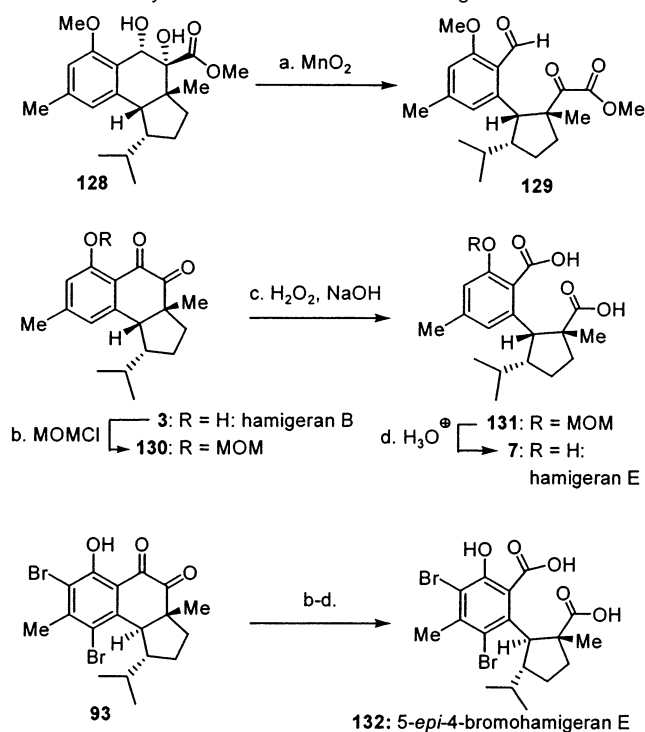


**Scheme 12.** Oxidative Cleavage of Hydroxy Ketone **96** to Diketone **122** and Ring-Contracted Ketone **123**<sup>a</sup>

<sup>a</sup> Reagents and conditions: (a) aqueous KOH, MeOH, 70 °C, 2 h; (b)  $n\text{Bu}_4\text{N}^+\text{IO}_4^-$  (2.0 equiv), dioxane, 100 °C, 1 h, varied yields (**122**, 10–50%, + **123**, 10–40%); (c)  $\text{BBr}_3$  (10.0 equiv),  $\text{CH}_2\text{Cl}_2$ ,  $-78^\circ\text{C}$ , 3 h, 86%.

aerobic conditions. In this novel cascade, initial saponification of the methyl ester (the generated carboxylic acid can be detected by TLC) is rapidly followed by a decarboxylation event and, finally, autoxidation, with the net result of the keto hydroxy ester of **2** being converted to the diketone functionality of **3** in 87% overall yield. Careful investigation of this reaction revealed the following aspects: (a) oxygen gas is necessary for good conversion; (b) the free phenolic group is essential for clean, room-temperature reaction; (c) the nature of the base is important to some extent. Finally, **4** was generated from **3** by NBS-facilitated introduction of the required second bromine atom (94% yield). The spectroscopic data for all four synthetic hamigerans **1–4** matched those reported for the natural substances, and so did their optical rotations, confirming both their absolute structures and enantiopurities.<sup>4</sup>

In our initial attack on the hamigeran B series, we utilized the periodate-based oxidative cleavage protocol, which gave considerable amounts of a side product which was characterized as the intriguing ring-contracted hamigeran analogue **123** (Scheme 12). Careful monitoring of the reactions involved revealed that compound **122** was formed initially and then transformed slowly into **123**, although the yields were low and rather erratic. It was, however, soon realized that this ring contraction was a photo-induced process, proceeding under UV irradiation consistently and in high yield (**122**  $\rightarrow$  **123**, 87% yield) as shown mechanistically in Scheme 13. This process is presumed to proceed via a Norrish type I fragmentation to afford diradical **126**, which, upon expulsion of a molecule of carbon monoxide followed by intramolecular recombination, furnished ring-contracted product **123** via diradical **127**. Interestingly, debromohamigeran B (**124**), in which the methyl protecting group on the phenol has been removed, fails to undergo this fragmentation reaction, being stable under the irradiation conditions. Hydrogen bonding between the phenolic OH and the proximal carbonyl group may be responsible for the

**Scheme 13.** Proposed Mechanism for the Decarbonylative Ring Contraction of **122** to **123****Scheme 14.** Synthesis of **7** and Related Analogues **129** and **132**<sup>a</sup>

<sup>a</sup> Reagents and conditions: (a)  $\text{MnO}_2$  (20 equiv),  $\text{CH}_2\text{Cl}_2$ , 25 °C, 2 h, 90%; (b) (MOM)Cl (2.5 equiv),  $i\text{Pr}_2\text{NEt}$  (3.5 equiv),  $\text{CH}_2\text{Cl}_2$ , 0 °C, 0.5 h, 76%; (c) 30% aqueous  $\text{H}_2\text{O}_2$ –dioxane–2 M aqueous NaOH (1:8:2), 0 °C, 10 min, 70%; (d) 3 M aqueous HCl–THF (1:1), 25 °C, 3 h, 70%.

deactivation of the 1,2-diketone system toward this photolytic rupture.

With the hamigerans A (**1** and **2**) and B (**3** and **4**) at hand, we then turned our attention to other members of the hamigeran family (Scheme 14). Thus, when vicinal diol **128** was exposed to activated  $\text{MnO}_2$ , a clean oxidative cleavage was observed, leading to keto aldehyde **129** (90% yield). This intermediate may lead to hamigeran C (**5**; see Figure 1), although this goal was not pursued at this juncture. Instead, we targeted **7** as shown in Scheme 14. Thus, MOM protection of **3** with (MOM)Cl and  $\text{Et}_3\text{N}$  led to diketone **130** in 76% yield. The latter compound (**130**) was subjected to oxidative cleavage with basic hydrogen peroxide in a biphasic medium (2 M aqueous NaOH– $\text{H}_2\text{O}_2$  in

dioxane, 10 min, 0 °C), and the crude reaction mixture was acidified (3 M aqueous HCl) prior to chromatographic purification on acid-washed silica gel, furnishing pure **7** via its MOM derivative **131** in 50% overall yield from **130**. The same sequence of reactions was applied in the conversion of **93** to 5-*epi*-4-bromohamigeran E (**132**) in similar overall yield. The <sup>1</sup>H NMR signals in the spectra of both compounds **7** and **132** were broad, presumably due to restricted rotation around the bond linking the two rings, a phenomenon that was somewhat suppressed by using wet CD<sub>3</sub>CN as solvent and running the spectra at 70 °C. Even under those conditions, however, the signals were still noticeably broad, and several of the quaternary carbons were not observable in the <sup>13</sup>C NMR spectrum. Despite this, **7** and **132** were fully characterized as pure compounds, confirming their structures. It should be noted that, even though compound **7** was identified as a natural product,<sup>4a</sup> this is the first time it was isolated in pure form.

### Conclusion

The described PEDA and IMPEDA chemistry opens new avenues to complex molecular frameworks via photo-induced cascade reactions. Its generality and scope has been explored

and demonstrated convincingly, while its applicability to natural product synthesis has been illustrated in a compelling manner. Stereochemical features of the IMPEDA process were characterized and parlayed into a successful asymmetric synthesis of several naturally occurring hamigerans (**1–4**) and analogues thereof. Further studies employing the developed chemistry toward compound library construction and chemical biology studies are both warranted and viable.

**Acknowledgment.** This work was financially supported by the National Institutes of Health, The Skaggs Institute for Chemical Biology, a Louis R. Jabinson fellowship (to D.L.F.G.), and grants from Amgen, Merck, and Pfizer.

**Note Added after ASAP Posting.** There was an error in the Scheme 4 reagents and conditions in the version posted on 12/17/03; the corrected version was posted on 1/6/04.

**Supporting Information Available:** Experimental procedures and compound characterization. This material is available free of charge via the Internet at <http://pubs.acs.org>.

JA030498F